Electronic Properties of the Axial Co−C and Co−S Bonds in B_{12} Systems − A Density Functional Study

Lucio Randaccio,*[a] Silvano Geremia,[a] Mauro Stener,[a] Daniele Toffoli,[a] and Ennio Zangrando*[a]

Keywords: Cobalamines / Coenzymes / Density functional calculations / X-ray diffraction

The numerous accurate structural data of cobalamins now available allows us to optimize the geometry of these systems, based on a simplified model by using density functional theory (DFT) calculations. This approach, which reproduces the trend of the experimental distances derived from EXAFS and X-ray crystal structures in the corrin macrocycle, permit us to interpret the electronic properties in the NB3–Co–X axial system. In particular, the results are analyzed for cobalamins containing a sulfur ligand which exhibits a "regular" *trans* influence, i.e., when the Co–S bond shortens, the *trans* Co–NB3 bond lengthens. This feature appears in contrast with an anomalous effect ("inverse" *trans* influence) postulated a few years ago by analyzing the structural data of several alkylcobaloximes, $LCo(DH)_2R$, a simple B_{12} model, and attributed principally to the electronic properties of the alkyl group R. The present study on the NB3–Co–S fragment does not indicate that the "inverse" *trans* influence is a general rule in cobalamins. The accurate crystal structures of the $[(SO_3)Cbl](NH_4)$ and [(thiourea)Cbl](PF_6) cobalamins based on synchrotron diffraction data at 100 K are also reported for comparison with the theoretical study. The former crystal structure, including one co-crystallized glycerol molecule, presents "for the first time" an ordered hydrogen-bonding pattern for the solvent molecules.

Introduction

Methionine synthase, whose cofactor is methylcobalamin (MeCbl; R = Me; Scheme 1) catalyzes the conversion of homocysteine to methionine.[1] The MeCbl-based enzymes (methyltransferases) catalyze the transfer of methyl groups from a nitrogen atom of methyltetrahydrofolate to cob(I)alamin (to form MeCbl) for onward transmission to an S atom of homocysteine. The enzymatic scheme proposed for the methionine synthase requires a reversible heterolytic cleavage of the Co−Me bond in the methyl carbocation and the strongly nucleophilic cob(I)alamin species.[2] In order to interpret the MeCbl function, several reactions of thiolates with organocobalt B_{12} model complexes have been carried out. However, the reports of these reactions were controversial.[3] Alkylthiolate cobalamin complexes, RS−Cbl, are also of interest as analogues of the RS and Co^{II}Cbl radical pair involved[4] in the mechanism of the coenzyme B_{12} (AdoCbl) dependent ribonucleotide reductase.[5]

Hence, knowledge of the properties and the behavior of thiolate−cobalamins is of significant interest. However, few thiolates have been isolated and characterized so far, and these have been principally by EXAFS[6] and NMR spectroscopy,[7,8] the former study also including (HSO_3)Cbl.

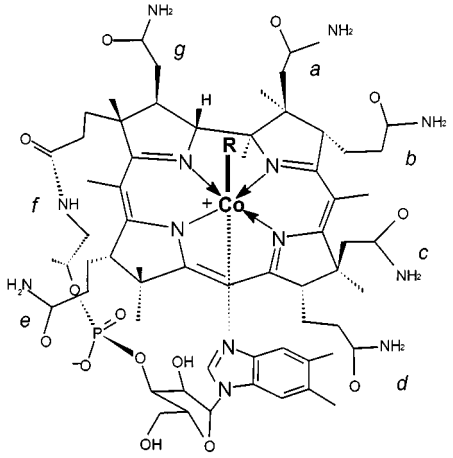

Scheme 1. Cobalamin

Only recently has the structural characterization of the NB3−Co−S fragment in $[(SO_3)Cbl](NH_4)$ (**1**) and $[(NH_2)_2CSCbl]Cl$ (**2**) been reported.[9]

Combining EXAFS and crystallographic results, it was concluded[6] that the S-containing ligands, such as thiolates and HSO_3^- have a weak *trans*-influencing ability, similar to that of H_2O[10] or CN.[11] Inversely, SO_3^{2-} exerts a strong *trans* influence similar to that of the methyl group.[9]

[a] Dipartimento di Scienze Chimiche, Università di Trieste
Via Giorgieri 1, 34127 Trieste, Italy
Fax: (internat.) + 39-040/676-3903
E-mail: zangrando@univ.trieste.it

  1434−1948/02/0101−0093 $ 17.50+.50/0

In order to verify the *trans* influence of HSO_3^-, we tried to prepare (HSO_3)Cbl according to a previous report.[6] The successive crystallographic analysis, described here, revealed that the compound is better formulated as $[(SO_3)Cbl](NH_4)$·glycerol solvate (**3**). Furthermore, in order to provide a more widespread comparison, the structural determination of $[(NH_2)_2CSCbl](PF_6)$ (**4**), more accurate than that of **3**, is also reported.

It is clear that the understanding of the chemical behavior of cobalamins requires an in-depth study of their electronic properties. However, despite the numerous experimental results, only a few attempts to understand their behavior on theoretical grounds have been carried out so far, principally on simple models[12] and in a few instances on R(Co−corrin)base (Scheme 2).[13] These studies, sometimes reaching conflicting conclusions, have been based on semiempirical approaches.[14] More recently, density functional theory (DFT) has been applied to calculate the geometry of some alkyl(Co−corrin)bases [15,16] and Co−corrin.[17] Furthermore, up to a few years ago, structural data on cobalamins were too low in accuracy for meaningful comparisons to be made.[18] Here, we report a theoretical approach, based on application of the density functional theory to the simplified model X(R)(Co−corrin)Bzm (Bzm = 5,6-dimethylbenzimidazole, X = R if alkyl group; Scheme 2), since the accurate structural data of several cobalamins is now available.[9−11,19,20] To complement this theoretical approach, which compares, for the first time, the electronic properties of the Co−S and Co−C bonds in the corrin model of cobalamins, some relationships with accurate structural data are reported.

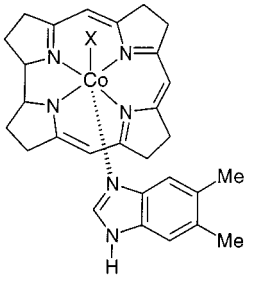

Scheme 2. Model corrin system used for calculations

Crystallographic Results

Crystal Packing

The cobalamin molecules are packed in their crystals in such a way as to form large cavities, in which solvent molecules are located (or ionic species when present, as in ClCbl·2LiCl[20]). These cavities may be described as being made by a central channel, running along a crystallographic 2_1 axis, and connected to side pockets at intervals defined by this axis.[19] The channel content is characterized by a disordered pattern of water molecules, while an ordered scheme of full-occupancy water molecules characterizes the pockets.[19]

Moreover, the crystal packing of isomorphous cobalamins can be divided into four clusters (I−IV),[9,18] according to the *c*/*a* and *b*/*a* ratios of the unit cell parameters. Isostructural cobalamins, which belong to the same cluster, display very similar amide side chain conformations,[9] and hence a closely related arrangement of solvent molecules within the pocket. Cobalamin **3** has unit cell parameters very similar to those of **1**, in spite of the presence of one glycerol molecule per Co atom and, hence, it still belongs to cluster I, which is characterized by an intramolecular H bond between the amide chain *c* and the axial sulfite ligand. Analogously, cobalamin **4** belongs to cluster II, as does $[(NH_2)_2CSCbl]Cl$ (**2**), and it does not exhibit any intramolecular H bond, the chain *c* points away from the axial thio-

Table 1. Hydrogen-bond scheme of water molecules (Ow), glycerol oxygen atoms (Og) and NH_4^+ within the pocket of compound **3**

	Occupancy	H bonds	H donors	H acceptors
Og1			Ow11	O3
Og2			N40	O44
Og3			N29, Ow9, Ow14	O1
NH_4^+		4		O4P, O62, O8R, O39
Ow1		3	N52	Ow2, O58
Ow2		3	Ow1	Ow3, O5P
Ow3		4	Ow2, O7R	O4P, Ow4
Ow4		4	Ow3, N59	O62, Ow12
Ow6		4	Ow7, Ow12 [Ow13]	Ow9, O33
Ow7		4	O8R, Ow8 [Ow15]	Ow6, Ow15 [Ow8]
Ow8		2 (3)	[Ow7]	O44, Ow7 [O6R]
Ow9		3	Ow6	O3, Og3 [Ow14]
Ow10	0.5	4	Ow11, Ow15 [Ow12]	O51, Ow12 [Ow15]
Ow11		4	N29, N45	Ow10, Og1
Ow12	0.59(2)	3	Ow4, Ow10	Ow6
Ow13	0.41(2)	2	Ow14 (?)	Ow6
Ow14	0.5	3 (?)	Ow9	Ow13 (?), Og3
Ow15		3	Ow7 [Ow10]	O39, Ow10 [Ow7]

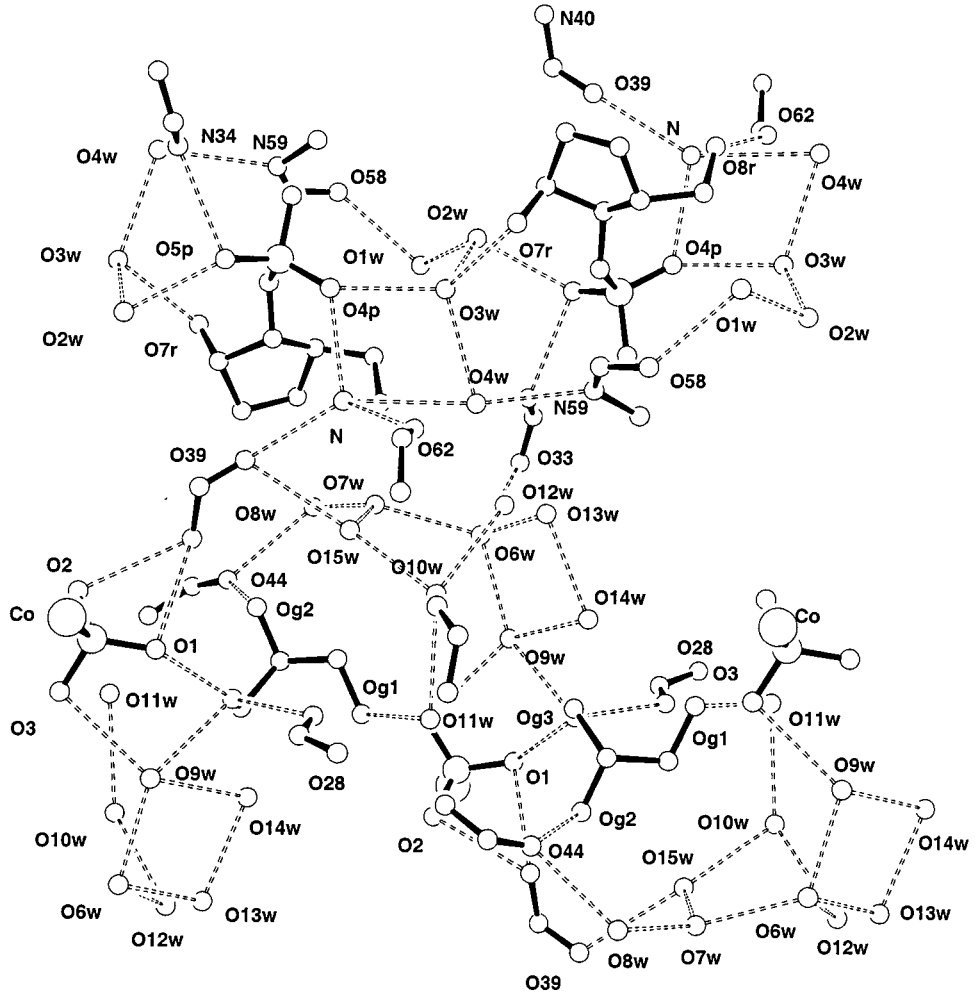

Figure 1. Hydrogen-bonding scheme (dashed lines) within the pocket for **3**; the content of a portion of the channel, running approximately along the horizontal direction of the figure, is also shown

urea ligand. The proposed H-bond scheme for **3** is given in Table 1 and the scheme within the cavity is shown in Figure 1. The structure within the pocket essentially corresponds to that found in **1** (see Figure 2 of ref.[9]), with only slight modifications (involving Ow3, Ow4, and OR7), as might be expected from the H-bond donor/acceptor scheme found in the crystal structure of vitamin B_{12r}, determined by neutron diffraction.[21] The glycerol molecules and the SO_3^{2-} groups are located within the channel, *where for the first time in a cobalamin crystal structure, the solvent molecules exhibit an ordered H-bond pattern*.

The H-bonding scheme within the cavity of **4** is significantly more detailed than that found in **2**, showing an ordered arrangement of the water molecules with full occupancy in the pocket and a disordered one in the channel, as has usually been the case in cobalamin crystal structures reported thus far. Of the disordered PF_6^- anion, the species with the highest occupancy (0.65) is located in the interface region, whereas the lower one (0.35) is in the channel.

Molecular Structure

The ORTEP drawings of **3** and **4** are shown in Figure 2 and Figure 3, respectively, and coordination distances are given in Table 2, where they are compared with those detected in the crystal structures of **1** and **2**. The folding angles, φ, defined as the dihedral angle between the two best-fit planes through N21/C4/C5/C6/N22/C9/C10 and C10/C11/N23/C14/C15/C16/N24, are also given in Table 2.

The axial distances in **1** and **3** are similar, whereas the Co−NB3 and Co−S distances are longer in **4** with respect to those of **2**. While the low accuracy of the latter structure[9] justifies the difference in the Co−NB3 distances, the discrepancy is more evident in the Co−S bond lengths. Actually, a re-examination of the difference Fourier map of **2** revealed a peak, along the Co−S bond, which could be assigned to a partially occupied (0.27) oxygen atom of a water ligand. This affected the previous refinement, which resulted in an artificial shortening of the Co−S distance.

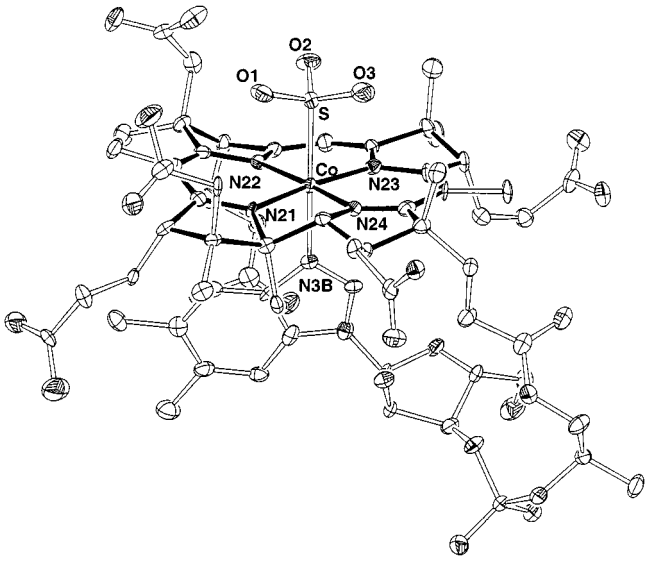

Figure 2. ORTEP drawings of **3** (thermal ellipsoids drawn at 50% probability level); solid bonds indicate the corrin ring

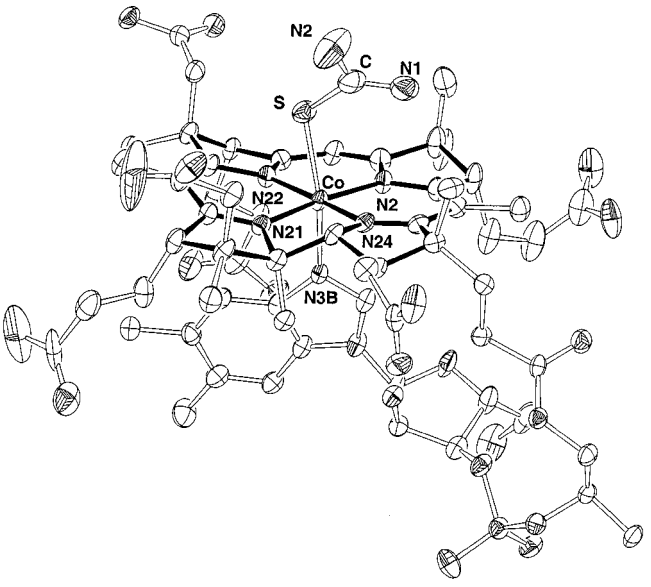

Figure 3. ORTEP drawings of **4** (thermal ellipsoids drawn at 30% probability level); solid bonds indicate the corrin ring

Table 2. Coordination distances [Å] and folding angle φ [°] in (SO_3)Cbl (**1**, **3**) and $(NH_2)_2$CSCbl (**2**, **4**)

	1	3	2	4
Co−S	2.231(1)	2.241(2)	2.216(7)	2.300(2)
Co−NB3	2.134(4)	2.156(5)	2.01(1)	2.032(5)
Co−N21	1.870(3)	1.883(5)	1.853(9)	1.884(5)
Co−N22	1.913(2)	1.911(5)	1.894(9)	1.916(4)
Co−N23	1.890(3)	1.904(5)	1.91(1)	1.926(5)
Co−N24	1.886(4)	1.901(5)	1.881(9)	1.895(4)
φ	16.3(1)	16.5(2)	14.9(3)	14.5(1)

Comparison of data confirms the previous finding that the Co−NB3 distance in the sulfite derivative is significantly longer than that in the thiourea analogue. On the other hand, the Co−S distance in the latter is about 0.06 Å longer than the corresponding values in **1** and **3**. Therefore, our previous conclusion,[9] that the Co−SO_3 and Co−$SC(NH_2)_2$ bond lengths were very similar, must be revised.

The sulfite geometry in **3** is characterized by S−O distances in the range 1.459(5)−1.490(5) Å and by approximately tetrahedral angles around S, which do not differ significantly from those found in **1** (Table 3). The orientation of SO_3 with respect to the equatorial plane appears to be determined by the intramolecular H bond [3.001(8) Å] between O2S and the NH_2 group of the amide chain *c*. In **4**, the Co−S−C angle is 118.9(3)° and the approximately planar S−$C(NH_2)_2$ group is oriented with respect to the equatorial moiety in such a way that the N21−Co−S−C and Co−S−C−N2 torsion angles are 107.1(4) and −143.7(8)°, respectively. The thiourea N1 atom is involved in a H bond with a water molecule [N1···Ow9 [2.99(1) Å].

The value of 10^7 of the equilibrium constant for the substitution of water by sulfite in aquocobalamin,[22] and the close similarities of the Co−SO_3 fragment geometry in **1** and **3**, strongly suggest the [(SO_3)Cbl](NH_4) formulation for **3**. Furthermore, the site assigned to the NH_4^+ ion corresponds to that occupied by K^+ in the isostructural CNCbl·KCl,[11] which belongs to the same cluster I. In addition, it has been claimed that (HSO_3)Cbl may be prepared from aquocobalamin,[6] by dissolving it in sodium acetate buffer (pH = 5) and adding sodium sulfite.[23] Thus, these results appear to favor the (HSO_3)Cbl formulation for **3**, assuming that the ammonium cation position is occupied by a water molecule (as found in **4**). However, this appears unlikely because of the four H-bond short contacts around this site (2.886, 2.734, 2.800, and 2.796 Å with O39, OP4, O62, and OR8, respectively, Table 1) should require a water molecule to be involved in bifurcate (probably long) H bonds. An early report[24] indicated that in acetate buffer at pH = 5.0, the complex exists as sulfitocobalamin, as evidenced by both IR spectroscopy (which showed no significant change over a pH range of 4−14) and electrophoresis (which indicates an overall charge of −1). Finally, the calculated geometry for the HSO_3^- group does not reproduce the experimental data as it does for the thiourea derivative (see below).

Discussion

Comparison of X-ray (XRD) and EXAFS Results

Several accurate X-ray structural determinations of the axial distances in cobalamins are now available.[9−11,19,20] Comparison with those previously determined by EXAFS may be useful in order to establish the reliability of bond lengths determined solely by using the first-shell Fourier filter analysis of EXAFS data.[6,25] In particular, such a comparison is important in view of the recent controversial EX-

Table 3. Calculated and experimental bond lengths [Å] and angles [°] of the Co−SO_3 fragment in **1** and **3** and of the Co−$SC(NH_2)_2$ in **4**; the calculated geometry for the HSO_3^- derivative is also reported

	1	**3**	calcd.	HSO_3 calcd.		**4**	calcd.
S−O1	1.466(4)	1.487(5)	1.469	1.625	S−C	1.724(8)	1.705
S−O2	1.452(4)	1.459(5)	1.461	1.440	C−N1	1.32(1)	1.321
S−O3	1.472(4)	1.490(5)	1.465	1.445	C−N2	1.31(1)	1.330
Co−S−O1	108.5(1)	108.6(2)	104.5	105.6	Co−S−C	118.9(3)	116.5
Co−S−O2	108.6(2)	108.5(2)	101.9	111.5	S−C−N1	122.3(7)	124.7
Co−S−O3	109.0(2)	108.4(2)	104.0	108.2	S−C−N2	116.6(7)	115.8
O1−S−O2	109.5(2)	110.2(3)	115.0	102.8	N1−C−N2	121.1(8)	119.4
O1−S−O3	109.4(3)	109.8(3)	115.4	107.1			
O2−S−O3	111.9(3)	111.4(3)	113.8	120.5			

AFS results concerning the considerable lengthening of the Co−N axial bond (by about 0.3 Å) in the protein-bound B_{12} coenzyme with respect to the free coenzyme.[26,27] In molecular biology, EXAFS is an ideal complement to biocrystallography in establishing the coordination distances in metalloenzyme and, under favorable circumstances, it can give coordination distances with an accuracy of 0.01 Å.[28] However, the analysis generally furnishes several solutions,[26] often difficult to interpret without comparison with accurate X-ray structural data, which often cannot be obtained for metalloproteins. Thus, such a dramatic impasse may be overcome if a model with precisely determined structure is available. Comparison of data for cobalamins, reported in Table 4, shows that the equatorial Co−Neq distances obtained by EXAFS and XRD are very similar. In fact, those determined by EXAFS range from 1.88(1) to 1.91(1) Å,[6] very close to the mean value of 1.895 Å based on 14 accurate X-ray structural determinations of R(X)−Cbl.[11] On the other hand, differences between axial distances, determined by means of EXAFS and XRD, range from −0.14 to +0.22 Å (Table 4). Thus, for example, the trend of the *trans* influence of the R(X) group, derived from EXAFS spectroscopy, is completely different. Such a large discrepancy has been ascribed to the presence of the four equatorial nitrogen atoms, which limits the accuracy of the axial distances because their contribution to the EXAFS spectrum interferes with that of the axial ligands.[27,29] The treatment of EXAFS data with the global mapping technique[26] has solved such a discrepancy in the case of $(H_2O)Cbl^+$, although it has been pointed out that multiple solutions are generally possible.[27,29] Thus, for $(H_2O)Cbl^+$, an alternative solution gave Co−N and Co−O distances in agreement with the crystallographic results (Table 4). More recently, an improvement of the global mapping technique, which reduces the parameters/observables ratio, has been proposed for the interpretation of EXAFS spectra of simple cobaloximes, a B_{12} model.[29] However, the lack of any structural information may sometimes render the choice among different solutions difficult.

Table 4. Cobalamins Co−X and Co−NB3 axial distances [Å] determined by X-ray diffraction (XRD) and EXAFS with relative differences Δ; the references in the footnotes correspond to XRD and EXAFS data, respectively

X	Co−X XRD	Co−X EXAFS	Δ	Co−NB3 XRD	Co−NB3 EXAFS	Δ
H_2O[a][b]	1.952(2)	1.90(2)	−0.05	1.925(2)	2.14(3)	0.22
H_2O[c]		1.97(2)	0.02		1.89(2)	−0.03
CN[d][b]	1.886(4)	1.90(3)	0.01	2.041(3)	2.15(3)	0.11
SO_3[e][f]	2.236(2)	2.35(2)	0.11	2.145(5)	2.16(4)	0.02
Me[b][d]	1.979(4)	2.00(3)	0.02	2.162(4)	2.20(3)	0.04
Ado[g][c]	2.033(4)	2.03(2)	0.00	2.237(3)	2.19(1)	−0.05
Cob(II)-alamin[h][i]	–	–	–	2.13(2)	1.99(3)	−0.14

[a] Ref.[10] – [b] Ref.[25]; EXAFS study based on a first shell Fourier filter analysis. – [c] Ref.[26]; EXAFS analysis based on a global mapping technique. – [d] Ref.[11] – [e] Mean value from structural data of **1** and **3**. – [f] Ref.[6]; the EXAFS study, based on a first shell Fourier filter analysis, refers to $(HSO_3)Cbl$. – [g] Ref.[32] – [h] B. Kräutler, W. Keller, C. Kratky, *J. Am. Chem. Soc.* **1989**, *111*, 8936−8938. – [i] I. Sagi, M. D. Wirt, E. Chen, S. Frisbie, M. R. Chance, *J. Am. Chem. Soc.* **1990**, *112*, 8639−8644.

DFT-Optimized Geometry

Calculated and experimental coordination distances for several cobalamins are reported in Table 5. As expected,[30] calculated distances are shorter than the experimental ones, with the exception of the axial distances of the sulfite derivative and, to a lesser extent, of the Co−OH_2 and Co−CF_3 distances. The relatively enormous lengthening of the calculated axial distances in the SO_3^{2-} derivative corresponds to large deviations from the tetrahedral value for the angles about the sulfur atom (Table 3). In fact, calculated Co−S−O (in the range 101.9−104.5°) and O−S−O angles (in the range 113.8−115.4°) are larger and smaller, respectively, than the experimental ones. This inconsistency in the geometry can be attributed to the repulsion of the negatively charged oxygen atoms of SO_3^{2-}. Analogous comparison for the thiourea derivative does not show any discrepancy (Table 3). Calculations carried out for the HSO_3^- derivative also indicate that "addition" of a proton to SO_3^{2-} decreases the O···O repulsion, reducing the angular distortion in the $CoSO_3$ fragment. If the calculated values for the latter are considered, instead of those of sulfite, the experimental trend of the axial distances, when X is varied, is very

Table 5. Experimental (at 100 K) and calculated coordination distances [Å] for several cobalamin derivatives; experimental data from ref.[11], if not otherwise stated

X	Co−NB3		Co−X		Co−N21		Co−N24		Co−N22		Co−N23	
	exp.	calcd.	exp.	calcd.	exp.	calcd.	exp.	calcd.	exp.	calcd.	exp.	calcd.
H_2O	1.925(2)	*1.881*	1.952(2)	*1.964*	1.881(2)	*1.858*	1.879(2)	*1.844*	1.897(2)	*1.886*	1.904(2)	*1.895*
Cl	1.981(3)	*1.972*	2.252(1)	*2.193*	1.873(3)	*1.847*	1.880(3)	*1.829*	1.902(3)	*1.892*	1.914(3)	*1.898*
CN[a]	2.041(3)	*2.002*	1.886(4)	*1.823*	1.881(3)	*1.840*	1.883(3)	*1.848*	1.911(3)	*1.882*	1.920(3)	*1.903*
CF_3[d]	2.05(1)	*2.051*	1.88(1)	*1.929*	1.870(9)	*1.842*	1.917(9)	*1.836*	1.95(1)	*1.888*	1.89(1)	*1.898*
Me	2.162(4)	*2.100*	1.979(4)	*1.942*	1.877(4)	*1.835*	1.874(4)	*1.829*	1.922(4)	*1.885*	1.918(4)	*1.890*
CMe_3	–	*2.174*	–	*2.082*	–	*1.833*		*1.822*		*1.895*		*1.898*
$SC(NH_2)_2$, **4**	2.032(5)	*1.974*	2.300(2)	*2.241*	1.884(5)	*1.853*	1.895(4)	*1.833*	1.916(4)	*1.901*	1.926(5)	*1.898*
SMe	2.04[b]	*2.028*	2.26[b]	*2.228*	–	*1.842*	–	*1.827*	–	*1.895*	–	*1.898*
HSO_3	–	*2.071*	–	*2.171*	–	*1.850*	–	*1.833*	–	*1.894*	–	*1.891*
SO_3[c]	2.145(5)	*2.170*	2.236(2)	*2.293*	1.877(4)	*1.840*	1.888(4)	*1.823*	1.912(4)	*1.875*	1.897(4)	*1.887*
Mean					1.878	*1.844*	1.888	*1.832*	1.916	*1.889*	1.910	*1.896*
Δ					0.014	*0.025*	0.043	*0.026*	0.053	*0.026*	0.036	*0.016*

[a] The calculated and experimental C−N bond lengths and Co−C−N angles are 1.166, 1.161(5) Å, and 175.4, 178.2(3)°, respectively. – [b] Estimated values (see text). – [c] Experimental mean values from structural data of **1** and **3**. – [d] X. Zou, K. L. Brown, *Inorg. Chim. Acta* **1998**, *267*, 305−308.

well reproduced. Thus it seems likely that the longer values of the calculated axial distances in $(SO_3)Cbl^-$ are due to a calculation artifact, ascribable to the high negative charge localized on the sulfite O atoms. This excess of charge should be caused by the lack, in the model molecule employed in calculations, of the interactions with the solvent (via H bonds), which delocalize the partial negative charge in the real system. This artifact gives rise to a strong apparent repulsion between the O atoms, indicated in the calculated structure by the flattening of the S tetrahedron towards the equatorial moiety (Table 3), which, in turn, enhances the steric repulsion with the macrocycle and provokes a lengthening of the Co−S bond, as well as a flattening of the corrin ligand (steric *cis* influence). In fact, the calculated folding angle φ of 10.26° [14.12° for $(HSO_3)Cbl$], is significantly smaller than the experimental one of 16.4° in the sulfite derivative. Consequently, the benzimidazole group is repelled away from the corrin with a concurrent lengthening of the Co−NB3 distance (steric *trans* influence).

The plots of calculated Co−NB3 and Co−X distances against the corresponding experimental values show fairly linear trends, excluding the calculated values for SO_3^{2-} (Figure 4). It should be stressed that in the simplified model of the corrin ligand used in the present calculations, H atoms have replaced the side groups. This does not allow consideration of the intramolecular interactions of the axial ligands with the corrin side chains. These interactions, such as the intramolecular H bonds between X and the corrin side chain *c* (when present), could affect the axial distances to some extent. It is of interest to compare the calculated axial distances for CN and Me derivatives of Table 5 with those obtained by Jensen et al.[16] by DFT calculations using the B3LYP method. These authors have found Co−C distances only marginally longer (ca. 0.03 Å), but Co−NB3 distances about 0.2 Å longer, than those calculated by our method.

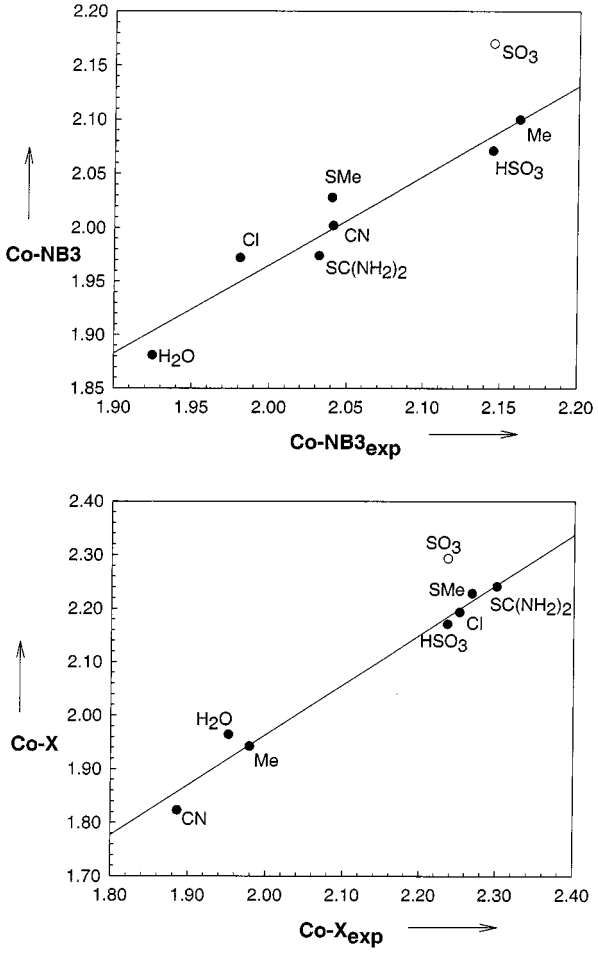

Figure 4. Plot of calculated Co−NB3 and Co−X distances [Å] in cobalamins vs. the corresponding experimental values; only experimental distances with e.s.d. values < 0.005 Å have been included (the experimental value of SO_3 is used also for HSO_3, see text)

Table 6. Calculated corrin distances [Å] in the XCo(corrin)Bzm system (X = H_2O and Me_3C) and in the Co^{II}(corrin), in comparison with experimental mean values from highly accurate structural data for several cobalamins

	H_2O[a]	Me_3C[a]	Co^{II}(corrin)[b]	Cbl(exp)[c]
Co−N21, Co−N24	1.858, 1.844	1.833, 1.822	1.85	1.878(3), 1.889(2)
Co−N22, Co−N23	1.886, 1.895	1.895, 1.898	1.90	1.907(3), 1.907(4)
N21−C1, N24−C19	1.457, 1.462	1.458, 1.454	1.49	1.500(6), 1.486(2)
C1−C2, C18−C19	1.516, 1.510	1.513, 1.513	−[d]	1.580(4), 1.530(4)
C2−C3, C17−C18	1.526, 1.529	1.527, 1.527	1.54	1.567(4), 1.560(5)
C3−C4, C16−C17	1.490, 1.491	1.493, 1.493	1.51	1.517(2), 1.535(4)
N21−C4, N24−C16	1.296, 1.298	1.295, 1.297	1.32	1.294(3), 1.300(2)
C1−C19	1.502	1.502	1.52	1.543(3)
C4−C5, C15−C16	1.412, 1.407	1.408, 1.407	1.41	1.444(4), 1.442(4)
C5−C6, C14−C15	1.360, 1.369	1.364, 1.364	1.37	1.363(3), 1.368(2)
N22−C6, N23−C14	1.373, 1.369	1.369, 1.368	1.39	1.401(3), 1.397(2)
N22−C9, N23−C11	1.336, 1.342	1.337, 1.338	1.37	1.340(3), 1.345(4)
C6−C7, C13−C14	1.488, 1.490	1.492, 1.495	1.51	1.545(3), 1.520(3)
C7−C8, C12−C13	1.520, 1.518	1.520, 1.517	1.53	1.550(2), 1.550(4)
C8−C9, C11−C12	1.482, 1.484	1.487, 1.487	−[d]	1.508(3), 1.512(4)
C9−C10, C10−C11	1.377, 1.374	1.374, 1.374	1.38	1.372(4), 1.386(3)

[a] Present work. − [b] Ref.[17]; a C_2 symmetry has been assumed in these calculations. − [c] Ref.[11] − [d] Missing data in ref.[17]

The experimental trend of the equatorial distances is well reproduced, with the Co−N21 and Co−N24 distances shorter than the Co−N22 and Co−N23 (Table 5). The calculated distances within the equatorial Co−corrin moiety are essentially unaffected by the axial ligands. In Table 6 a comparison for X = CMe_3 (the strongest σ-donating and bulkiest group) and for X = H_2O (the weakest σ-donating and the less bulky one) is reported. The C_2 symmetry of the corrin unit is quite well preserved, with differences in the symmetry equivalent to distances not exceeding 0.008 Å for X = H_2O, and 0.004 Å for X = CMe_3. The comparison of corrin distances shows no significant influence of the X axial ligand, since the differences between analogous distances also do not exceed 0.008 Å. However, the deviation from planarity, signified by φ values of 16.91 and 6.82° for the H_2O and CMe_3 derivatives, respectively, reflects the bulk of the axial ligand.

The trend of the experimental distances in the delocalized moiety of the corrin (Scheme 2) is fairly well reproduced (Table 6). The calculated values of the C−C single bonds of the pyrrole rings are shorter, by 0.02−0.06 Å, than those determined experimentally, the larger differences involve the more "crowded" bonds, such as C_q-C_q, where C_q represents a quaternary C atom. These discrepancies should be ascribed to the simplified equatorial ligand used in the calculations. This cannot reproduce the *steric pressure exerted by the side chains which lengthen in cobalamins the corrin C−C single bonds.*[10] On the contrary, the expected trend (short−long−short distances) in the pyrrole fragment $C(sp^2)-C(sp^3)-C(sp^3)-C(sp^2)$ is well reproduced.

It is interesting to compare the present results with those of Rovira et al.[17] derived by means of density functional molecular dynamics within the Car−Parrinello scheme for the square-planar Co(corrin), assumed to have C_2 symmetry. It was found that the corrin distances were not influenced at all by the oxidation state +1 ($S = 0$), or +2 ($S = 1$) of the metal center. The calculated distances reproduced the experimental trend in the delocalized moiety of the corrin (Table 6). As expected, the pyrrole C−C single bonds were shorter, to a greater or lesser extent, than the experimental ones, but longer than our calculated values, by about 0.02 Å. On the contrary, the calculated Co−N equatorial distances of the present work compare well with those of Rovira. Therefore, the axial ligands do not appear to influence the equatorial distances, as suggested by those authors.[17]

Electronic Properties of the Co−C and Co−S Bonds

Mullikan populations (MP) on the NB3−Co−X fragment are given in Table 7. As it is well known, Mulliken population analysis allows a partial charge to be attributed to a particular atom in a molecule. This procedure is not rigorous, since there is not a physical definition of the atomic charge within a molecule; however, it can be very helpful for interpretative purposes.[31]

Table 7. Mullikan population on the NB3−Co−X fragment for several cobalamins X-Cbl

X	NB3	Co	X
H_2O	−.4673	.7290	.2842
Cl	−.4757	.4524	−.2269
CN	−.4874	.5280	−.3270
CF_3	−.4924	.4311	−.0416
Me	−.5000	.5449	.0726
CMe_3	−.4966	.6481	.1029
$SC(NH_2)_2$	−.4781	.3813	.7247
SMe	−.4844	.3745	.0792
HSO_3	−.4862	.3205	.1737
SO_3	−.4952	.3308	−.4111

The only linear relationship is found between MP of NB3 and the calculated Co−NB3 distances, as shown in Figure 5 for several X groups. The trend of the Mulliken charge on the NB3 group, reported in Table 7 is surprising to some

extent, especially if the observed random fluctuation of the charge on Co and X group is considered. This behavior may be rationalized if we consider the nature of the chemical bonds in which the metal atom is involved. In fact, while the NB3 group is always connected to the Co atom, preserving the nature of the atom pair, the nature of the atom of the X group connected to Co varies and it is therefore more difficult to compare the Mulliken charges on Co and X groups along the series. Apart from the stability of the Mulliken charge on NB3, it is interesting to observe that the negative charge increases when the *trans* influence of the X group becomes higher. This finding is consistent with a model of the NB3−Co chemical bond in terms of electronic charge donation from the nitrogen atom to the metal ion. In fact, the NB3−Co distance increases with the increase of the *trans* influence of X, and consequently the weakening of the latter bond leaves an excess of negative charge on the NB3 atom.

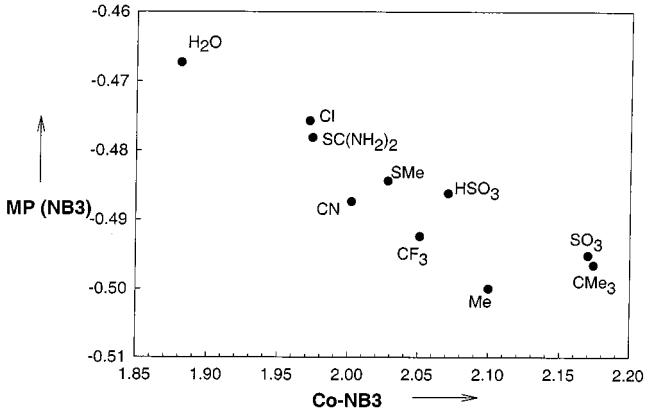

Figure 5. Plot of Mullikan population (MP) on NB3 vs. the calculated Co−NB3 distances [Å] for several X groups

Some peculiarities of the Mulliken charges on Co and X are worth noting. First, the positive charge of the metal ion is lower (< 0.4 au) when the Co is bound to a sulfur atom of the X group, irrespective of the position of the system along the series of increasing *trans* influence. This behavior can be explained by the "soft" character of the sulfur atom, which may be seen as an "electron reservoir" and is therefore able to screen more effectively the positive metal charge than the other ligands. The second interesting point is the very high positive charge of the thiourea. This finding clearly indicates that a strong conjugation is present in this ligand between the lone pairs of N and the C−S double bond. The latter is further polarized by the presence of the positive metal ion, which should enhance the conjugation via a Co−S π donation to the metal ion. Finally, the third observation regards the very high negative charge (−0.41 au) present on the SO_3 group. It has already been pointed out that the theory does not compare favorably with experimental data for this system, as previously described.

The NB3−Co−SR Fragment

Recently, we have found a good linear relationships between the Co−N and Co−X axial distances in cobalamins in comparison with the corresponding variables in cobaloximes, $LCo(DH)_2R$ (where DH = monoanion of dimethylglyoxime, L = neutral Lewis base, R = alkyl group).[11] This allowed an evaluation of the Co−NB3 and Co−SMe distances in cobalamins.[9] On the basis of these linear equations, slightly modified by including the recent data of the more accurate structures of MeCbl, CNCbl,[11] and AdoCbl,[32] ($r^2 = 0.980$, $n = 6$ for the Co−S bond and $r^2 = 0.966$, $n = 7$ for the Co−NB3 bond) the Co−SMe and Co−NB3 distances are found to be 2.26 and 2.04 Å, respectively. During the preparation of the present manuscript, we became aware of an accurate structural determination of (γ-glutamylcysteinyl)cobalamin (GCS-Cbl),[33] where the Co−S and Co−NB3 bond lengths were found to be 2.267(2) and 2.049(6) Å, respectively. These values are very close to those predicted above.

When X = HSO_3^-, SMe, and $SC(NH_2)_2$, the trend for the calculated Co−NB3 distances (Table 5) is as follows:
$SC(NH_2)_2$ (1.974) < SMe (2.028) < HSO_3^- (2.071 Å)
Inversely, the Co−S distances increase in the opposite order:
$SC(NH_2)_2$ (2.241) > SMe (2.228) > HSO_3^- (2.171 Å)

The above trends give an example of a "regular" *trans* influence, which is when the Co−S bond shortens and the Co−NB3 bond lengthens. A plot of the Co−NB3 vs. Co−S distances is reported in Figure 6. Correspondingly, the positive charge on Co (MP) decreases with the lengthening of the Co−NB3 distance, but it increases with the Co−S bond, shortening from $SC(NH_2)_2$ to HSO_3^- (Figure 7, bottom).

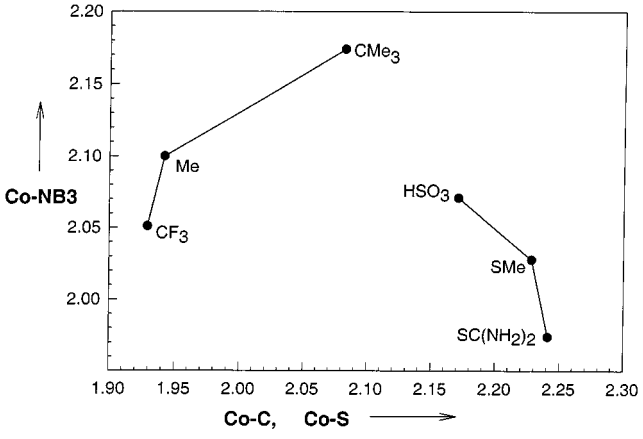

Figure 6. Plot of calculated Co−NB3 distances vs. the corresponding Co−X distances [Å] in cobalamins with alkyl and sulfur ligands

On the other hand, an "inverse" *trans* influence (i.e. both the Co−NB3 and Co−R distances increase) has been found[15] when the σ-donating ability of the R group increases from CN to Et. This finding was obtained by DFT calculations applied to the same simplified model corrin we have used in the present calculation.

Although the present Co−NB3 distances are approximately 0.15 Å shorter (and even more) than those calculated

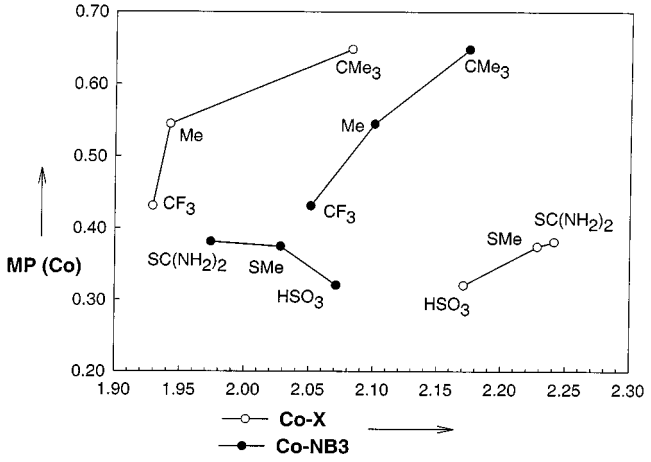

Figure 7. Plot of the Mullikan population (MP) on cobalt vs. the calculated axial bond lengths in cobalamins with alkyl (upper) and sulfur ligands (bottom)

by Andruniow et al.,[15] we have found this "inverse" *trans* influence for R = CF_3, Me and CMe_3 (Figure 6 and Table 5). Consistently, the positive charge on Co significantly increases with the lengthening of both the Co−NB3 and Co−C bonds (Figure 7, top). These findings appear to suggest that the different trend of the charge on Co with axial distances, in the two series containing S and C ligands, may be related to the "regular" or "inverse" *trans* influence of Figure 6. In fact, in the "regular" *trans* influence, the increase of the σ donation of the L group is reflected by the decrease of the Co positive charge. Therefore, the effect appears to be electronic in nature. On the other hand, in the "inverse" *trans* influence the positive metal charge increases with the σ-donating power of the R group. Thus, it cannot be an electronic, but rather a steric effect, due to the larger dimension of the σ-donor group (CMe_3). The steric repulsion, caused by the bulk of R, lengthens both the Co−R (steric *cis* influence) and Co−Nax (steric *trans* influence) distances and consequently the σ donation from ligands to the metal decreases, leading to a more positively charged metal.

The "inverse" *trans* influence, derived through an analysis of structural data in several alkylcobaloximes, $LCo(DH)_2R$, a simple B_{12} model,[34] was attributed principally to the electronic properties of R. However, it has been shown that in these complexes the bulk of R (independently of its electronic properties) also contributes significantly in determining the Co−R distance, because of its interaction with the equatorial ligand.[35] In fact, compared to the Me analogue, alkylcobaloximes with strong electronic withdrawing and bulky R groups, such as $CH(CN)CH_2CN$,[36] and $CF(CF_3)_2$,[37] show a significant lengthening of the Co−C bond (up to 0.08 Å) and a shortening of the Co−L bond (up to 0.03 Å). The present analysis of the NB3−Co−S fragment geometry does not support the idea that the "inverse" *trans* influence is a general rule also in cobalamins.

Experimental Section

Materials: Commercial samples of $(H_2OCbl)Cl$, stated purity by manufacturer about 96%, were purchased from Fluka. The other reactants were reagent grade and used without further purification. The complexes $[C_{62}H_{88}CoN_{13}O_{17}PS](NH_4)\cdot 12(H_2O)$ $(C_3H_8O_3)$ (**3**) and $[C_{63}H_{92}CoN_{15}O_{14}PS](PF_6)\cdot 13.3(H_2O)$ (**4**) were prepared in situ, growing the single crystals by the hanging drop method of vapor diffusion.

Preparation of 3: 2 μL of an aqueous $(H_2OCbl)Cl$ solution at 25 mg/mL was mixed with 2 μL of the precipitant solution containing $(NH_4)_2SO_4$, 20% glycerol, and 0.06 M $NaHSO_3$. Typical concentration range for precipitants were 20−45% in $(NH_4)_2SO_4$. Suitable single crystals were obtained only with 45% $(NH_4)_2SO_4$. Addition of LiCl did not result in formation of crystals. Attempts with PEG (with or without LiCl) were unsuccessful. The formation of the sulfite derivative, starting from $NaHSO_3$, is due to the high formation constant ($pK = -7$, with respect to the aquocobalamin) of $(SO_3)Cbl^-$, which allows its formation even in acid conditions (pH close to 4), where the concentration ratio $[HSO_3^-]/[SO_3^{2-}]$ is about 1000.

Preparation of 4: Several attempts to grow high quality single crystals were carried out, exploiting the procedure previously described,[10] slightly modified by addition of $(NH_4)PF_6$ in the ranges 0.10−0.50 M (by 0.05 M steps) and 0.05−0.16 M (by 0.01 M steps) and by substituting $(NH_4)_2SO_4$ with 20% glycerol as precipitant agent. Single crystals were obtained when 2 μL of an aqueous $(H_2OCbl)Cl$ solution at 25 mg/mL was mixed with 2 μL of the precipitant solution $(NH_4)PF_6$ (0.13 M), 20% glycerol and 0.30 M thiourea.

X-ray Structural Determinations: Diffraction experiments were carried out at the X-ray diffraction beamline of the Elettra Synchrotron, Trieste (Italy), using the rotating crystal method. Data were collected on a 345 mm MAR image plate with crystals mounted in loops and frozen to 100 K using a nitrogen-stream cryo-cooler. Crystallographic data for **3** and **4** are given in Table 8. The diffraction data were integrated using the DENZO program [38] and reflections subsequently were scaled and merged using the SCALEPACK program.[38] Friedel equivalent reflections were not merged and no absorption correction was applied. The phase problem was solved using the coordinates of an isomorphous structure as a starting model. The structural parameters were refined by full-matrix least squares on F^2 for all data using SHELXL-97.[39] The Fourier and Fourier difference maps clearly indicated that in **3** the PF_6^- anion is disordered over two different sites with occupancy factors of 0.65 and 0.35. Final *R* factors and details of refinements are reported in Table 8. Crystallographic data (excluding structure factors) for the structures reported in this paper have been deposited with the Cambridge Crystallographic Data Centre as supplementary publication, CCDC-161809 (**3**) and -161810 (**4**). Copies of the data can be obtained free of charge on application to CCDC, 12 Union Road, Cambridge CB2 1EZ, UK [Fax: (internat.) + 44-1223/336-033; E-mail: deposit@ccdc.cam.ac.uk].

Computational Method: The electronic structures of the systems under study were determined by solving the Kohn−Sham equations,[40] in the framework of Density Functional Theory (DFT), employing the ADF suite of quantum chemistry packages.[41,42] The simplified model for the corrin ligand, shown in Scheme 2, was used as in previous calculations.[13,15] During the SCF procedure, the Local Density Approximation (LDA) to the exchange correlation energy functional was applied, accordingly to the Vosko, Wilk

Table 8. Crystal data and structure refinement parameters of compounds **3** and **4**

	3	**4**
Empirical formula	$C_{65}H_{124}CoN_{14}O_{32}PS$	$C_{63}H_{118.60}CoF_6N_{15}O_{27.30}P_2S$
Formula mass	1735.74	1790.06
Crystal system	orthorhombic	orthorhombic
Space group	$P2_12_12_1$	$P2_12_12_1$
a [Å]	16.125(5)	15.758(4)
b [Å]	20.827(8)	22.698(4)
c [Å]	24.515(4)	24.765(7)
V [Å^3]	8233(4)	8858(4)
Z	4	4
$\rho_{calcd.}$ [g cm^{-3}]	1.400	1.342
μ [mm^{-1}]	0.345	0.345
Radiation, λ [Å]	synchrotron, 0.8558	synchrotron, 0.8558
$F(000)$	3704	3788
$2\theta_{max}$ [°]	54	56
No. reflns. total, unique	9932, 9267	12657, 12139
R(int.)	0.0523	0.0576
No. reflns $I > 2\sigma$ (I)	9139	11295
No. of parameters	1055	1103
Goodness-of-fit	1.045	1.054
$R1$[a]	0.0603	0.0778
$wR2$[a]	0.1763	0.2169

[a] $R1 = \Sigma||F_o| - |F_c||/\Sigma|F_o|$; $wR2 = [\Sigma w\,(|F_o|^2 - |F_c|^2)^2/\Sigma w(F_o^2)^2]^{1/2}$.

and Nusair VWN parameterization.[43] The basis set consisted of Slater Type Orbitals (STO) taken from the database of ADF: For all the atoms a Double Zeta plus Polarization (DZP) frozen core set was chosen, with the exception of the cobalt atom where, as suggested by a previous study,[30] the more extended Triple Zeta (TZ) frozen core was utilized. The geometry of the systems was optimized employing a quasi-Newton procedure with analytical energy gradients and default convergence criteria. Since we are mainly interested in the geometry of the systems, the VWN exchange-correlation potential was employed, which performs better and is more accurate for structural analysis than the more demanding GGA potentials, as has been already pointed out in a previous computational study on transition metal compounds.[30] A larger basis set (TZP) has been tested for the SO_3 group with the aim of improving the capability of the method in order to describe negative fragments with a diffuse electron density. However, we did not observe any improvement. It can therefore be concluded that the method employed gives reliable results, and that the cause of the disagreement with the experiment must be found elsewhere.

Acknowledgments

This work was supported by Ministero dell'Università e della Ricerca Scientifica e Tecnologica (Rome) (PRIN 9803184222).

[1] C. L. Drennan, M. M. Dixon, D. M. Hoover, J. T. Jarret, C. W. Goulding, R. G. Mattews, M. L. Ludwig, in Vitamin B_{12} and B_{12}-Proteins (Eds.: B. Kräutler, D. Arigoni, B. T. Golding), Wiley-VCH, Weinheim, **1998**, pp. 133−155.
[2] [2a] R. G. Matthews, J. T. Drummond, *Chem. Rev.* **1990**, *90*, 1275−1290. − [2b] R. G. Matthews, in Chemistry and Biochemistry of B_{12} (Ed.: R. Banerjee), J. Wiley & Sons Inc., New York, **1999**, pp. 681−706.
[3] S. M. Polson, L. Hansen, L. G. Marzilli, *Inorg. Chem.* **1997**, *36*, 307−313.
[4] N. E. Brasch, T.-L. C. Hsu, K. M. Doll, R. G. Finke, *J. Inorg. Biochem.* **1999**, *76*, 197−209.
[5] [5a] S. S. Licht, S. Booker, J. Stubbe, *Biochemistry* **1999**, *38*, 1221−1233. − [5b] S. Licht, G. J. Gerfen, J. Stubbe, *Science* **1996**, *271*, 477−481.
[6] E. M. Scheuring, I. Sagi, M. R. Chance, *Biochemistry* **1994**, *33*, 6310−6315.
[7] K. L. Brown, X. Zou, S. R. Savon, D. W. Jacobsen, *Biochemistry* **1993**, *32*, 8421.
[8] T.-L. C. Hsu, N. E. Brasch, R. G. Finke, *Inorg. Chem.* **1998**, *37*, 5109−5116. A preliminary structural analysis of the C_5F_5S−Cbl from this laboratory gave Co−S and Co−NB3 distances of 2.295(9) and 1.95(3) Å, respectively.
[9] L. Randaccio, S. Geremia, G. Nardin, M. Slouf, I. Srnova, *Inorg. Chem.* **1999**, *38*, 4087−4092.
[10] C. Kratky, G. Färber, K. Gruber, K. Wilson, Z. Dauter, H.-F. Nolting, R. Konrat, B. Kräutler, *J. Am. Chem. Soc.* **1995**, *117*, 4654−4670.
[11] L. Randaccio, M. Furlan, S. Geremia, M. Slouf, I. Srnova, D. Toffoli, *Inorg. Chem.* **2000**, *39*, 3403−3413.
[12] [12a] G. N. Schrauzer, L. P. Lee, J. W. Sibert, *J. Am. Chem. Soc.* **1970**, *92*, 2997−3005. − [12b] L. Salem, O. Eisenstein, N. T. Anh, H.-B. Burgi, A. Devaquet, G. Segal, A. Veillard, *Nouv. J. Chem.* **1977**, *1*, 335−348. − [12c] C. Mealli, M. Sabat, L. G. Marzilli, *J. Am. Chem. Soc.* **1987**, *109*, 1593−1594. − [12d] D. W. Christianson, W. N. Lipscomb, *J. Am. Chem. Soc.* **1985**, *107*, 2682−2686. − [12e] L. M. Hansen, P. N. V. Pavan Kumar, D. S. Marynick, *Inorg. Chem.* **1994**, *33*, 728−735.
[13] [13a] L. Zhou, N. M. Kostic, *Inorg. Chem.* **1987**, *26*, 4194−4197. − [13b] L. M. Hansen, A. Derecskei-Kovacs, D. S. Marynick, *J. Mol. Struct.* **1998**, *431*, 53−57.
[14] L. Randaccio, *Comments Inorg. Chem.* **1999**, *21*, 327−376.
[15] [15a] T. Andruniow, M. Z. Zgierski, P. M. Kozlowski, *Chem. Phys. Lett.* **2000**, *331*, 502−508; *Chem. Phys. Lett.* **2000**, *331*, 509−512. − [15b] T. Andruniow, M. Z. Zgierski, P. M. Kozlowski, *Chem. Phys. Lett.* **2000**, *331*, 509−512. − [15c] T. Andruniow, M. Z. Zgierski, P. M. Kozlowski, *J. Phys. Chem. B* **2000**, *104*, 10921−10927.
[16] K. P. Jensen, S. P. A. Sauer, T. Liljefors, P.-O. Norrby, *Organometallics* **2001**, *20*, 550−556
[17] C. Rovira, K. Kunc, J. Hutter, M. Parrinello, *Inorg. Chem.* **2001**, *40*, 11−17.
[18] K. Gruber, G. Jogl, G. Klintschar, C. Kratky, in *Vitamin B_{12}*

and B_{12}-Proteins (Eds.: B. Kräutler, D. Arigoni, B. T. Golding), Wiley-VCH, Weinheim, **1998**, pp. 335−347.
[19] [19a] J. P. Bouquiere, J. L. Finney, H. F. J. Savage, *Acta Crystallogr., Sect. B* **1994**, *50*, 566−578. − [19b] J. P. Bouquiere, J. L. Finney, M. S. Lehmann, P. F. Lindley, H. F. J. Savage, *Acta Crystallogr., Sect. B* **1993**, *49*, 79−89. − [19c] H. F. J Savage, *Biophysics* **1986**, *50*, 947−965. − [19d] H. F. J Savage, *Biophysics* **1986**, *50*, 967−980. − [19e] H. F. J. Savage, J. L. Finney, *Nature (London)* **1986**, *322*, 717−720.
[20] L. Randaccio, M. Furlan, S. Geremia, M. Slouf, *Inorg. Chem.* **1998**, *37*, 5390−5393.
[21] P. Langan, M. Lehmann, C. Wilkinson, G. Jogl, C. Kratky, *Acta Crystallogr., Sect. D* **1999**, *55*, 51−59.
[22] J. M. Pratt, in *B_{12} (Ed.: D. Dolphin), Wiley and Sons, New York, **1982**, vol. 1, p. 325−392.*
[23] E. Pezacka, R. Green, D. W. Jacobsen, *Biochem. Biophys. Res. Commun.* **1990**, *169*, 443−450.
[24] R. A. Firth, H. A. O. Hill, J. M. Pratt, R. G. Thorp, R. J. P. Williams, *J. Chem. Soc. A* **1969**, 381−386.
[25] I. Sagi, M. R. Chance, *J. Am. Chem. Soc.* **1992**, *114*, 8061−8066.
[26] E. M. Scheuring, R. Padmakumar, R. Banerjee, M. R. Chance, *J. Am. Chem. Soc.* **1997**, *119*, 12192−12200.
[27] F. Champloy, G. Jogl, R. Reitzer, W. Buckel, H. Boethe, B. Beatrix, G. Broeker, A. Michalowicz, W. Meyer-Klaucke, C. Kratky, *J. Am. Chem. Soc.* **1999**, *121*, 11780−11789.
[28] H. Bertagnolli, T. S. Ertel, *Angew. Chem.* ***1994***, *106*, 15−37; *Angew. Chem. Int. Ed. Engl.* **1994**, *39*, 45−66.
[29] E. Fonda, A. Michalowicz, L. Randaccio, G. Tauzher, G. Vlaic, *Eur. J. Inorg. Chem.*, **2001**, 1269−1278.
[30] M. Stener, M. Calligaris, *J. Mol. Struct. (Theochem)* **2000**, *497*, 91−104.
[31] A. Szabo and N. Ostlund, *Modern Quantum Chemistry*, Macmillan Publishing Co., New York, **1982**.
[32] L. Randaccio, et al., data from this laboratory, in preparation.
[33] R.G. Finke, private communication.
[34] D. J. A. De Ridder, E. Zangrando, H. B. Burgi, *J. Mol. Struct.* **1996**, *374*, 63−83.
[35] L. Randaccio, S. Geremia, E. Zangrando, C. Ebert, *Inorg. Chem.* **1994**, *33*, 4641−4650.
[36] J. P. Charland, W. M. Attia, L. Randaccio, L. G. Marzilli, *Organometallics* **1990**, *29*, 1367−1375.
[37] P. J. Toscano, H. Brand, S. Liu, J. Zubieta, *Inorg. Chem.* **1990**, *29*, 2101−2105
[38] Z. Otwinowski, W. Minor, *Methods Enzymol.* **1996**, *276*, 307−326.
[39] G. M. Sheldrick, *SHELXL-97, Program for Structure Refinement*, Universität Göttingen, Germany, ***1997***.
[40] R. G. Parr, W. Yang, in *Density Functional Theory of Atoms and Molecules* (Eds.: R. Breslow, J. B. Goodenough, J. Halpern, J. S. Rowllinson), Oxford University Press, New York, ***1989***.
[41] E. J. Baerends, D. E. Ellis, P. Ros, *Chem. Phys.* **1973**, *2*, 41.
[42] C. Guerra Fonseca, J. G. Snijders, G. te Velde, E. J. Baerends, *Theor. Chem. Acc.* **1998**, *99*, 391−403.
[43] S. H. Vosko, L. Wilk, M. Nusair, *Can. J. Phys.* **1980**, *58*, 1200.
Received July 6, 2001
[I01253]